OPEN

The local immune response during *Echinococcus granulosus* growth in a quantitative hepatic experimental model

Zhide Li[1,2,3,8], Chuanshan Zhang[3,4,8], Liang Li[5], Xiaojuan Bi[3], Liang Li[3], Shuting Yang[1,3], Ning Zhang[1,2], Hui Wang[1,3], Ning Yang[1,3], Abuduaini Abulizi[1,2], Abudusalamu Aini[1,2], Renyong Lin[3], Dominique A. Vuitton[6,7] & Hao Wen[1,2,3]*

The local immune mechanisms responsible for the establishment and development of *Echinococcus granulosus sensu stricto* infection in the liver, have been little explored. We developed a suitable experimental model that mimics naturally infected livers using portal injection of protoscoleces. Opposite to *Echinococcus multilocularis* infection which is dose-dependent, fully mature hydatid cysts can be established in the liver whatever the injection dose; although most of the infection sites were seen at the establishment phase as inflammatory granulomas associated with fibrosis, they never matured into cysts. At the establishment phase, a strong immune response was composed of T and B cells, with T1-type, T2-type cells and cytokines and IL-10-secreting CD8$^+$ T cells in the liver. At the established phase, results suggested a local production of antibodies by B cells, and an involvement of NK and NKT cells. Infection outcome and local immune response in the liver, were different in the mouse models of *Echinococcus granulosus sensu stricto* and *Echinococcus multilocularis* respectively; however, only early specificities at the microenvironment level might explain the major differences found between the lesions induced by the two species. Our quantitative experimental model appears fully appropriate to further study this microenvironment and its relationship with each cestode species.

Cystic echinococcosis (CE), a severe zoonosis caused by *Echinococcus granulosus sensu lato* (*E. granulosus s.l.*) larvae, is threatening human's health and social development worldwide[1,2]. CE presents in humans as a cyst, most frequently in the liver[3]. The metacestode is composed of the 'hydatid', a cystic structure composed, from inside to outside, of the hydatid fluid (HF), the germinal layer (GL) that produces the protoscoleces (PSCs), the laminated layer (LL), of parasitic origin, and the adventitial layer (AL) produced by the host's immune reaction. The treatments of CE consist of surgical resection, percutaneous drainage with injection of protoscolex-killing compounds (protoscolecides), and the anti-parasite drug, albendazole[4,5]. Host's immune system interact with *E. granulosus s.l.* through immune cells and cytokines which contribute to immediate or delayed healing or to the continuous growth of the cyst when infection has been successfully established[6]. The WHO classification of CE cysts in the liver highly reflects the outcome of such a metacestode-host interaction by defining three types of cysts: active (CE1 and CE2), transitional (CE3 a and b), and degenerating/inactive (CE4 and CE5). However, the mechanisms responsible for either self-healing (inactivation) or maintenance of a chronic infection have not been fully elucidated yet. From various studies performed in CE patients and in experimental models, it is commonly accepted

[1]State Key Laboratory of Pathogenesis, Prevention, Treatment of High Incidence Diseases in Central Asia, the First Affiliated Hospital of Xinjiang Medical University, Urumqi, Xinjiang, China. [2]Department of Hepatic Hydatid and Hepatobiliary Surgery, Digestive and Vascular Surgery Centre, the First Affiliated Hospital of Xinjiang Medical University, Urumqi, Xinjiang, China. [3]Xinjiang Key Laboratory of Echinococcosis, and WHO-Collaborating Center on Prevention and Care Management of Echinococcosis, Clinical Research Institute, the First Affiliated Hospital of Xinjiang Medical University, Urumqi, Xinjiang, China. [4]Basic Medical College, Xinjiang Medical University, Urumqi, Xinjiang, China. [5]Chronic Disease Laboratory, Institutes for Life Sciences and School of Medicine, South China University of Technology, Guangzhou, China. [6]French National Reference Center for Echinococcosis, Department of Parasitology, University Hospital, Besançon, France. [7]University Bourgogne Franche-Comté (EA 3181), Besançon, France. [8]These authors contributed equally: Zhide Li and Chuanshan Zhang. *email: Dr.wenhao@163.com

that CE cyst formation is mainly mediated by impairment of dendritic cells (DC) differentiation and maturation, and by the differentiation of specialized regulatory T cells and related cytokines such as Interleukin-10 (IL-10) and transforming growth factor beta (TGF-β)[7]. In addition, a feature of *E. granulosus s.l.* infection is its capacity to induce T helper 2 (Th2)-type response, which are beneficial to the survival of the metacestode, rather than T helper 1 (Th1) cytokines, capable of its destruction[8].

Previously, we developed a suitable experimental mouse model that mimics naturally infected livers by injection of *Echinococcus multilocularis* (*E. multilocularis*) PSCs via the portal vein. This model allowed us to study host's immune response according to the parasite load. By using this model, we demonstrated that local cellular immunity and fibrogenesis were actually protective and fully able to limit metacestode growth or even to clear it in the liver after low or medium dose-infection, while impairment of cellular immunity was followed by a more rapid and severe course of the disease in high dose-infected mice[9]. Recently, we have adapted this quantitative mouse model to *Echinococcus granulosus sensu stricto* (*E. granulosus s.s.*) to study the effect of innovative treatments of CE[10,11].

For obvious reasons, the local immune response before and at the early stages of cyst formation in human CE is barely known. Very little information is available on the local immune response and its course in the liver, at the early stages of *E. granulosus* infection in experimental models[12,13]. In addition, marked differences between pathology and clinical course of CE and AE have long been recognized[3,12] although *E. granulosus* spp. and *E. multilocularis* share most of their DNA sequences[14–16]. However, all immunological studies have shown that the course of T cell differentiation and cytokine secretion were highly similar in both infections, yet no clear immunological explanation has been provided up to now to render these differential pathological and clinical features[12]. Taking benefit from the similarity and quantitative nature of the model of PSC injection in the portal vein for both *E. granulosus* and *E. multilocularis*, we thus investigated the impact of the inoculation of different *E. granulosus s.s.* PSC numbers (corresponding to low, medium and high dose groups, respectively LDG, MDG and HDG) on the development of the cysts in the liver of C57BL/6 mice, a strain of intermediate susceptibility to both species of *Echinococcus*, as is observed in humans, and we assessed the relationship between the observed histological aspects, intensity of infection, and liver fibrosis. To study the relationship between infection following increasing number of PSCs and the host's immune response, and make the immunological profile observed in this model comparable to that previously described in the experimental model of *E. multilocularis* infection, we measured most of the known cellular and cytokine markers of the immune balance in *Echinococcus* spp. infection and analyzed whether and how these patterns affected the establishment of infection and parasite growth.

Results

Establishment of a mouse model by injecting different doses of *E. granulosus s.s.* PSCs via the portal vein.

General observation revealed that the hepatic cysts were embedded at the surface of the liver, or in the liver, or were (less frequently) free in the peritoneal cavity. The development of hepatic cysts was observed from the 4th to 24th week after infection; and different courses of infection could be seen in all dose groups (Supplementary Fig. S1). At 2 weeks, tiny white foci less than 1 mm in size were observed on the surface of the liver. Congestive hemorrhagic patches were also observed and an increased number of foci were seen from LDG, MDG to HDG at that stage, and there were no cysts in any of the groups, including HDG (2000 PSCs). At 4 weeks, the foci decreased in number, but the sizes of the foci were larger than those observed at 2 weeks by 1–2 mm. Cysts were seen in one mouse in HDG. At 8 weeks, cysts of 1–4 mm in diameter and 1–10 in number were found mostly at the margin of the liver lobes in MDG and HDG; cysts were observed in only one mouse in LDG (50 PSCs) (Supplementary Table S1). At 12 and 16 weeks, cysts of 1–10 mm in diameter and 1–20 in number were observed in all groups. At 20 and 24 weeks, numerous cysts of 1–15 mm in diameter were found in the liver of all mice whatever the group, and a few cysts in the peritoneal cavity were observed in HDG.

From the 8th week, as the doses of PSCs increased, the mean number of cysts gradually increased, but there was only a weak, albeit significant correlation between the number of cysts/mice and the dose of PSC injected (r = 0.22, R^2 = 0.05, $p < 0.05$) (Supplementary Table S1). In addition, as the dose of PSCs increased, the mean formation ratio of cysts gradually decreased (Supplementary Table S2). Most cysts were located in the caudate or left lobe of liver.

Histopathological features and types of lesions in the liver of mice with different *E. granulosus s.s.* PSC inocula.

At 2 weeks, lymphocytes infiltrated the *E. granulosus s.s.* inoculum in all infected groups, and a few foci were surrounded by fibroblasts; a few PSCs could still be observed in the portal vein. At 4 weeks, the cyst formed in a mouse of the HDG was typical with GL, LL and AL. At 8 weeks, when the cysts began to form in all groups and gradually increased in number, at the periphery of the lesion(s), numerous fibroblasts and inflammatory cells were present and an obvious increase of granulomas (inflammatory cells with fibrosis) was observed. From the 12th to 24th weeks, cysts were the main lesions and consisted of the GL, LL and AL composed of picric acid-Sirius red stained fibrosis and of host immune cells, including lymphocytes, macrophages, and epithelioid cells. Cysts were located at the edge of or inside the liver. Some of the cysts contained necrotic tissue. At that stage, the number and size of cysts in HDG were usually larger than that in MDG and LDG. (Fig. 1a).

As shown in Fig. 1b, inflammatory foci occurred most frequently at 2 and 4 weeks, inflammatory foci with fibrosis at 8 and 12 weeks, and infectious foci with cystic structures at 20 and 24 weeks. In all groups, fibrotic foci without inflammatory cell infiltration were rarely observed. In LDG, inflammatory foci decreased from 2 to 24 weeks (from 99.7% to 44.3%). Inflammatory foci with fibrosis increased from 2 weeks and peaked at 8 weeks (36.4% of all foci), then decreased at 24 weeks. Infectious foci with cystic structures appeared at 8 weeks, then gradually increased, and peaked at 20 weeks (54.9% of all foci). In MDG, the inflammatory foci were at the lowest level at 8 weeks (15.3% of all foci). Inflammatory foci with fibrosis increased and peaked at 8 weeks (74.5% of all infectious foci), then decreased at 24 weeks. Infectious foci with cystic structures also appeared at 8 weeks,
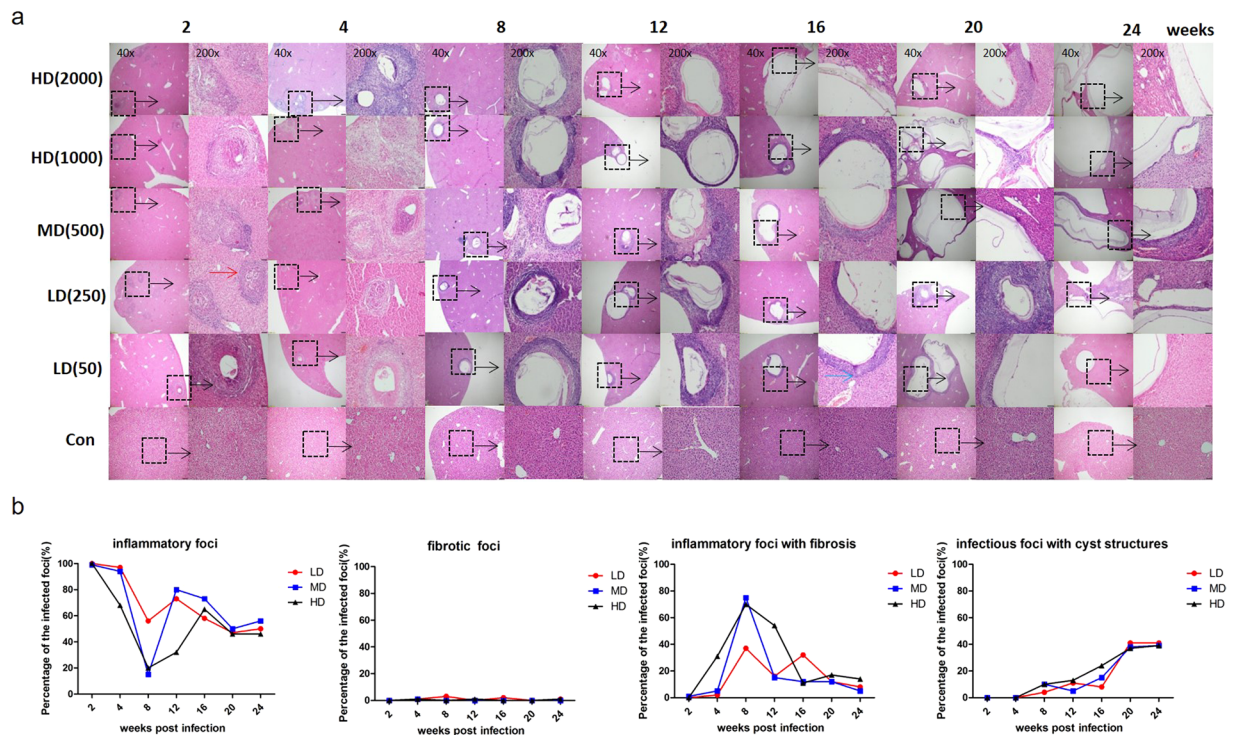
Figure 1. Hepatic histopathological alterations and granulomatous response in mice during the course of infection. (**a**) Histopathological alterations of the liver from mice infected with different PSC inocula during the course of infection. H&E staining of liver sections. The original magnification was at $40\times$, and the corresponding images on the right were magnified at $200\times$; bars indicate $200\,\mu m$ or $50\,\mu m$ in the $40\times$ or in the $200\times$ magnification images, respectively. Red arrow indicates inflammatory cell zone; Blue arrow indicates fibrosis areas. Dashed line marks the border of granuloma around the parasitic lesion in the infected group. (**b**) Hepatic granulomatous response to *E. granulosus* infection with different doses. Liver histological reaction at each infectious foci was scored as (1) inflammatory foci, parasite-free, except for possible PSC remnants, composed of macrophages, lymphocytes, and other inflammatory cells; (2) fibrotic foci, parasite-free, with no visible PSCs or cysts, only composed of fibrosis; (3) inflammatory foci with fibrosis, parasite-free, with no visible PSCs or cysts, only composed of granulomatous inflammation combined with liver fibrosis; (4) infectious foci, cystic structure composed of the germinal layer and laminated layer, surrounded with macrophages, lymphocytes, fibroblasts, myofibroblasts, as well as fibrosis (adventitial layer). All sizes of infectious foci were calculated via microscope examination of the liver including 4–6 mice per group. PSCs: protoscoleces. LD: 50 or 250 PSCs; MD: 500 PSCs; HD: 1000 or 2000 PSCs. Data are shown as mean $\pm$ standard error of the mean (SEM), $*p < 0.05$, $**p < 0.01$ and $***p < 0.001$.

increased gradually, and peaked at 20 weeks (56.9% of all infectious foci). In HDG, the course of the various types was similar to that observed in MDG. Inflammatory foci were at their lowest level at 8 weeks (18.4% of all infectious foci); inflammatory foci with fibrosis peaked at 8 weeks (66.9% of all infectious foci), and infectious foci with cystic structures peaked at 24 weeks (53.3% of all infectious foci).
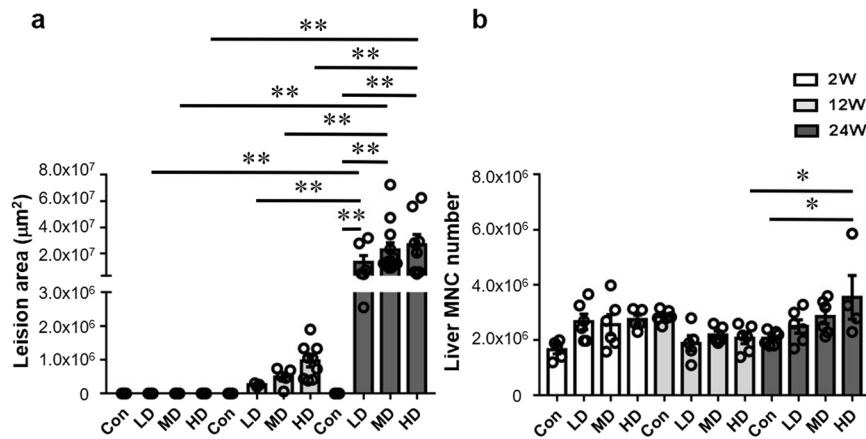
Lesion size and inflammatory cell infiltration in the liver of mice with different *E. granulosus* s.s. PSC inocula. No specific identified lesions were observed in the control groups, with sham injection of PSCs, at any post-injection time. At 2 weeks, there was no difference in the size of liver lesions. At 12 weeks, the size of liver lesions was not significantly different in the three groups. At 24 weeks, the average size of liver lesions in the three groups was significantly higher than at 2 and 12 weeks (Fig. 2a). At 24 weeks, the number of infiltrating mononuclear cells (MNCs) in the liver in HDG was significantly higher than in the control group, and also significantly higher than at 12 weeks post-injection (Fig. 2b).

Characteristics of hepatic fibrosis in mice with different *E. granulosus* s.s. PSC inocula. At 2 weeks, mild collagen deposition was observed around granulomatous inflammatory lesions and in the portal spaces, but it was not significantly different in all infected groups. At 12 and 24 weeks, picric acid-Sirius red staining, albeit higher in MDG and HDG than in LDG, was not significantly different in all infected groups. At these stages, collagen deposits were mainly localized around the LL of the cysts, and also in the granulomas without cyst formation (Supplementary Fig. S2a,b).

Cells with α-SMA expression were also present around the cysts and in the granulomas (Supplementary Fig. S2c). At 2 and 24 weeks, the percentage of α-SMA positive cells was significantly higher in HDG and MDG than in the control groups ($p = 0.0179$; $p = 0.0282$; $p < 0.001$; $p < 0.001$). At 24 weeks, the percentage of α-SMA

Figure 2. Lesion size and inflammatory infiltration in the liver of mice during the course of infection. (**a**) Liver lesion area determined by microscopic measurement of H&E-stained tissue sections, and expressed as square micrometers (μm^2). (**b**) Total number of hepatic mononuclear cells (MNCs). LD: 50 PSCs; MD: 500 PSCs; HD: 2000 PSCs. Data are shown as mean $\pm$ standard error of the mean (SEM, 4–6 mice per group), *$p < 0.05$, **$p < 0.01$ and ***$p < 0.001$.

positive cells was higher in HDG than in LDG ($p = 0.0216$). α-SMA positive cells were still present at the late stage of infection, and the percentage of α-SMA positive cells was higher in HDG and MDG at 24 weeks than at 12 weeks ($p = 0.0024$; $p = 0.0097$) (Supplementary Fig. S2d).

Lymphocyte composition in the liver of mice with different *E. granulosus s.s.* PSC inocula. The absolute numbers of CD4$^+$ T cells were significantly higher in HDG than in LDG at 2 weeks ($p = 0.003$), but the difference was not statistically signifcant at 12 and 24 weeks. The absolute numbers of CD4$^+$ T cells were significantly higher in HDG and MDG than in the control group at 2 weeks ($p < 0.001$; $p = 0.003$). The number of CD8$^+$ T cells was not different in the three groups at all three stages (Fig. 3a,b). The CD4$^+$/CD8$^+$ T cell ratio gradually increased in the liver as the infection dose increased, and it was markedly lower in LDG than in MDG and HDG at 2 weeks ($p < 0.001$; $p < 0.001$). Moreover, the ratio of CD4$^+$/CD8$^+$ T cells was significantly higher in MDG and HDG at 2 weeks than at 24 weeks ($p < 0.001$; $p < 0.001$) (Fig. 3c).

The number of NK cells was significantly lower in HDG at 12 weeks than at 2 and 24 weeks ($p = 0.0028$; $p = 0.0457$) (Fig. 3d). The number of NKT cells was significantly higher in LDG at 12 weeks than at 24 weeks ($p = 0.0386$), and higher in HDG at 24 weeks than at 12 weeks ($p = 0.0292$) (Fig. 3e). In addition, the absolute number of B cells was higher in LDG at 2 weeks than at 12 weeks ($p = 0.0011$); and it was higher in LDG than in HDG at 2 weeks ($p = 0.0457$) (Fig. 3f).

Phenotype of memory T cell subsets in the liver of mice with different *E. granulosus s.s.* PSC inocula. At 2, 12 and 24 weeks, the percentage of effector memory CD4$^+$ T cells (Tem, CD44$^+$CD62L$^-$) was higher in MDG and HDG than in LDG ($p < 0.001$; $p = 0.0177$), and it was significantly increased in MDG and HDG at 2 weeks, and represented $78.2 \pm 4.3\%$ of CD4$^+$ T cells in HDG (Fig. 4a and Supplementary Fig. S3).

At 2, 12 and 24 weeks, the percentage of central memory CD8$^+$ T cells (Tcm, CD44$^+$CD62L$^+$) was not significantly different in the three groups. In addition, it was higher in MDG at 24 weeks than at 12 weeks ($p = 0.0186$). The percentage of effector memory CD8$^+$ T cells (Tem, CD44$^+$CD62L$^-$) was higher in HDG than in LDG at 2, 12 and 24 weeks, and it was significantly different at 2 weeks ($p < 0.001$). In LDG, CD8$^+$ Tem percentage was higher at 12 than at 2 weeks ($p = 0.0037$). In MDG, CD8$^+$ Tem percentage was higher at 12 weeks than at 2 weeks ($p = 0.0039$). CD8$^+$ Tem percentage was significantly higher in HDG than in control group, and represented $48.2 \pm 6.1\%$ of CD8$^+$ T cells at 2 weeks ($p = 0.0017$) (Fig. 4b,c).

Dynamic changes of T1-type CD4 T cells and CD8 T cells in the liver of mice with different *E. granulosus s.s.* PSC inocula. T1-type CD4$^+$ T cells (CD4$^+$IFN-γ^+, CD4$^+$TNF-α^+) and CD8$^+$ T cells (CD8$^+$IFN-γ^+, CD8$^+$TNF-α^+) were investigated in the liver (Fig. 5 and Supplementary Fig. S4). In all three groups, despite some apparent changes in T1-type CD4$^+$ T cells and CD8$^+$ T cells percentages with time, these changes were not significant. However, in HDG, CD4$^+$IFN-γ^+T cells percentage was significantly higher at 12 weeks than at 2 and 24 weeks ($p = 0.0032$; $p < 0.001$).

At 2 weeks, CD4$^+$IFN-γ^+T cells percentage was significantly higher in HDG than in LDG ($p = 0.0453$). At 12 weeks, CD4$^+$IFN-γ^+T cells percentage was significantly higher in HDG than in LDG and MDG ($p < 0.001$; $p < 0.001$). At 24 weeks, CD8$^+$IFN-γ^+T cells percentage was significantly higher in HDG than in LDG and MDG ($p = 0.0045$; $p = 0.0011$).

CD8$^+$ TNF-α^+T cells percentage was significantly higher in HDG than in LDG at 2 weeks ($p = 0.0223$).

Dynamic changes of T2-type CD4 T cells in the liver of mice with different *E. granulosus s.s.* PSC inocula. T2-type CD4$^+$ T cells (CD4$^+$IL-4$^+$) were investigated in the liver (Fig. 5 and Supplementary Fig. S4).

a CD4⁺T cells

b CD8⁺T cells

c CD4⁺/ CD8⁺
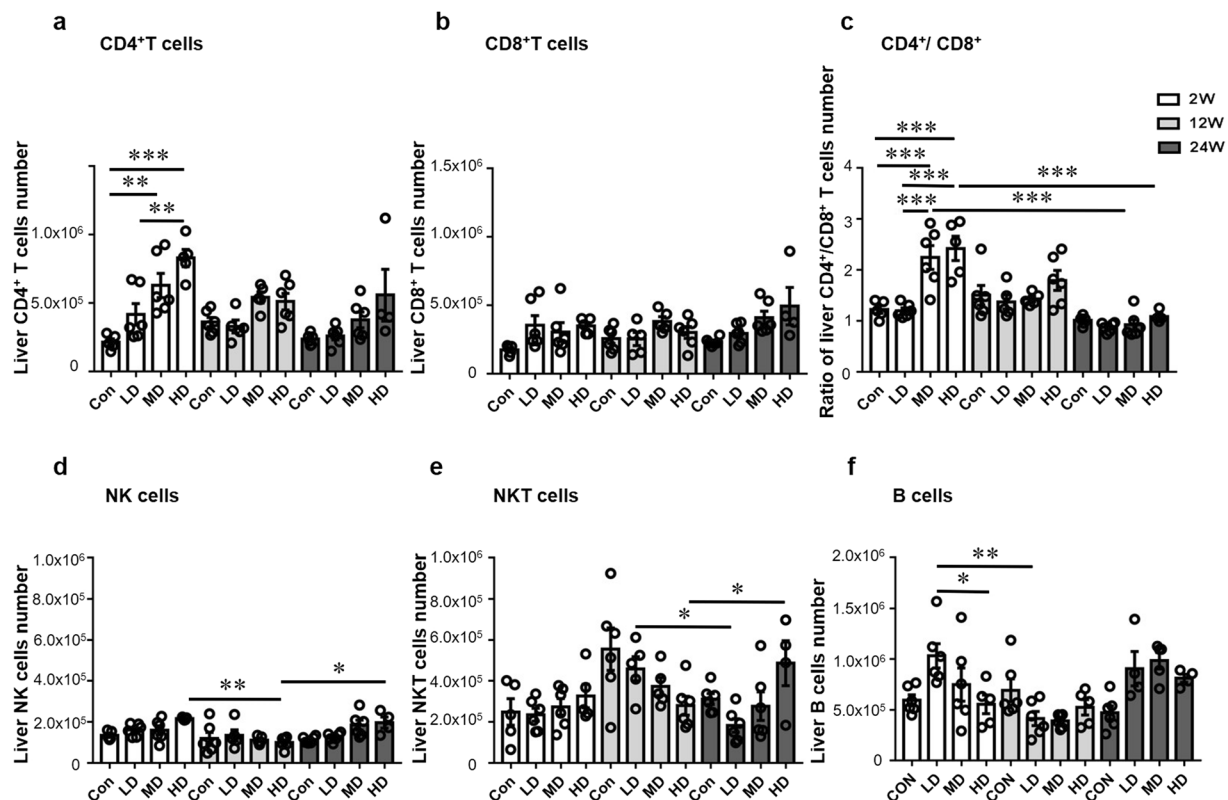
Figure 3. Inflammatory cell subsets in the liver of mice infected during the course of infection. (**a**) Absolute quantification of hepatic CD4 (NK1.1⁻CD3⁺CD4⁺) T cells. (**b**) Absolute quantification of hepatic CD8 (NK1.1⁻CD3⁺CD8⁺) T cells. (**c**) Ratio of CD4⁺ T cells/CD8⁺ T cells in the liver. (**d**) Absolute quantification of hepatic NK (NK1.1⁺CD3⁻) cells. (**e**) Absolute quantification of hepatic NKT cells. (**f**) Absolute quantification of hepatic CD19⁺ B cells. LD: 50 PSCs; MD: 500 PSCs; HD: 2000PSCs. Data are shown as mean ± standard error of the mean (SEM, 4–6 mice per group), *$p < 0.05$, **$p < 0.01$ and ***$p < 0.001$.
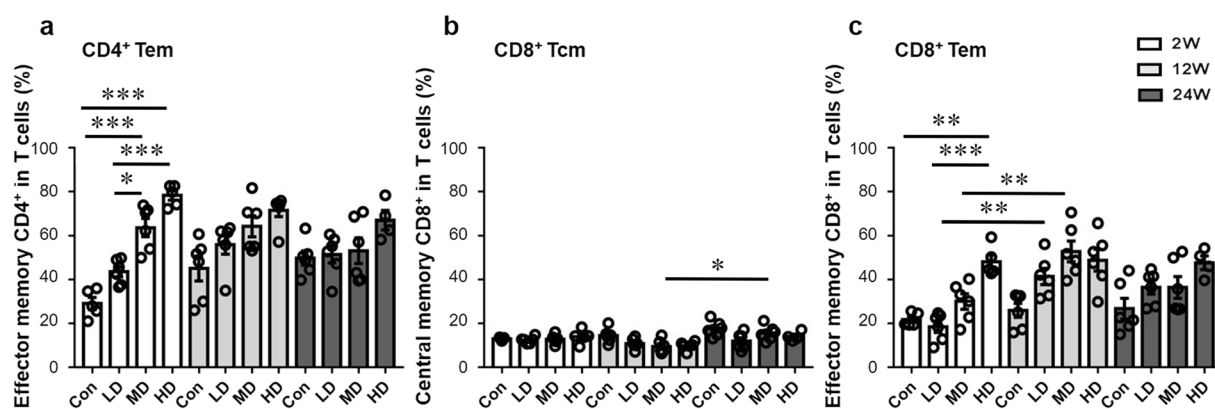
Figure 4. Memory T cell phenotypes in the liver of mice during the course of infection. (**a**) Percentage of effector memory CD4⁺ T cells (Tem, CD44⁺CD62L⁻)/CD4⁺ T cells in the liver. (**b**) Percentage of central memory CD8⁺ T cells (Tcm, CD44⁺CD62L⁺)/CD8⁺ T cells in the liver. (**c**) Percentage of effector memory CD8⁺ T cells (Tem, CD44⁺CD62L⁻)/CD8⁺ T cells in the liver. LD: 50 PSCs; MD: 500 PSCs; HD: 2000 PSCs. Data are shown as mean ± standard error of the mean (SEM, 4–6 mice per group), *$p < 0.05$, **$p < 0.01$ and ***$p < 0.001$.

In LDG, the percentage of T2-type cells gradually increased from the 2nd to the 12th week, then was lower at the 24th week. In HDG, the percentage of T2-type cells was significantly higher at 12 and 24 weeks than at 2 weeks ($p < 0.001$; $p = 0.0467$).
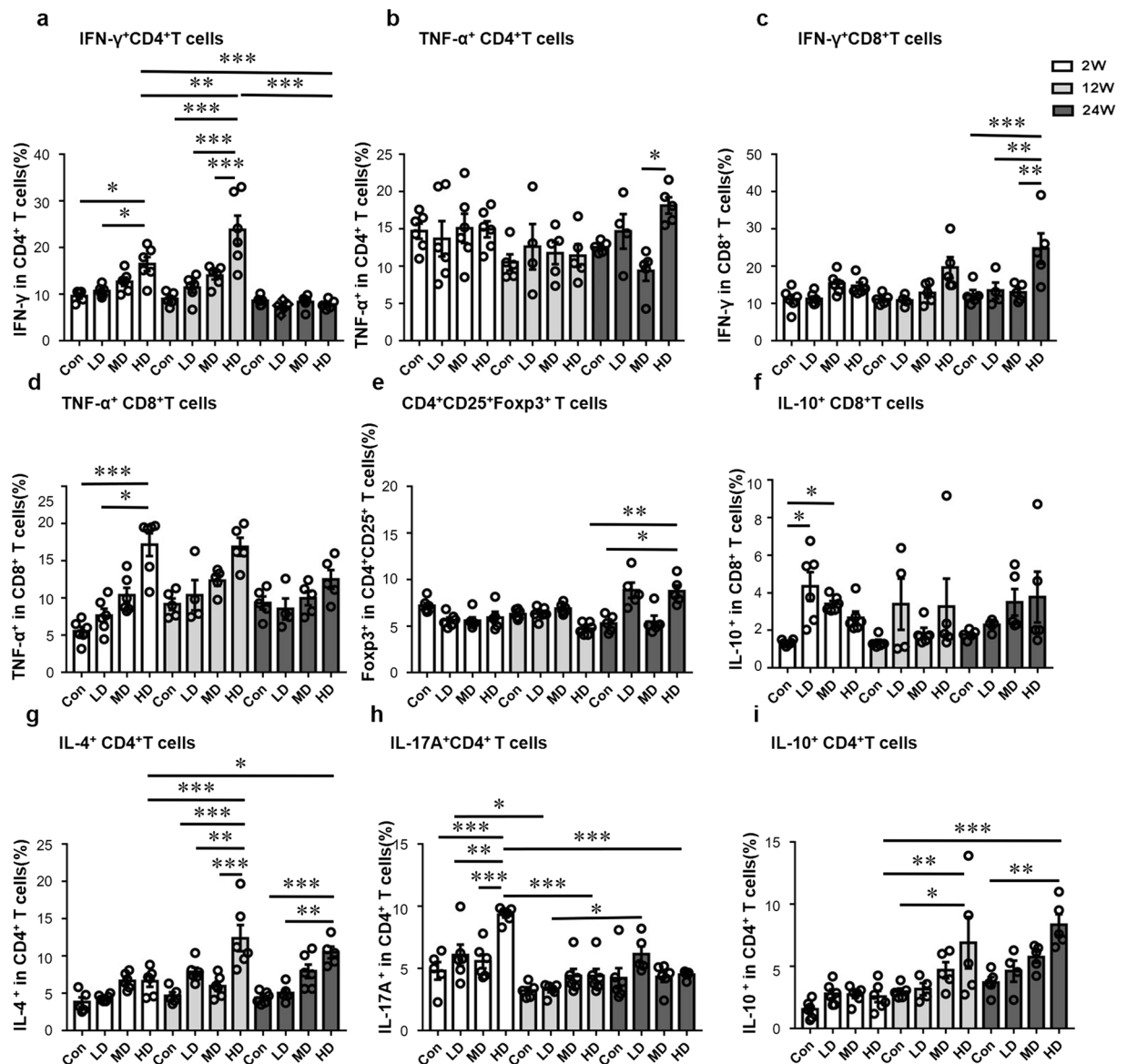
Figure 5. Distribution of T cell subsets in the liver of mice during the course of infection. (**a**) Percentage of CD4+IFN-γ+ T cells (T1-type)/CD4+ T cells in the liver. (**b**) Percentage of CD4+TNF-α+ T cells (T1-type)/CD4+ T cells in the liver. (**c**) Percentage of CD8+IFN-γ+ T cells (T1-type)/CD8+ T cells in the liver. (**d**) Percentage of CD8+ TNF-α+ T cells (T1-type)/CD8+ T cells in the liver. (**e**) Percentage of CD4+CD25+Foxp3+ T cells (Treg-type)/CD4+ T cells in the liver. (**f**) Percentage of CD8+IL-10+ T cells (Treg-type)/CD8+ T cells in the liver. (**g**) Percentage of CD4+IL-4+ T cells (T2-type)/CD4+T cells in the liver. (**h**) Percentage of CD4+IL-17A+ T cells (T17-type)/CD4+T cells in the liver. (**i**) Percentage of CD4+IL-10+ T cells (Treg-type)/CD4+T cells in the liver. LD: 50 PSCs; MD: 500 PSCs; HD: 2000 PSCs. Data are shown as mean ± standard error of the mean (SEM, 4–6 mice per group),*$p < 0.05$, **$p < 0.01$ and ***$p < 0.001$.

At 2 weeks, the percentage of T2-type cells was not significantly different among all groups. At 12 weeks, the percentage of T2-type CD4+ T cells was significantly higher in HDG than in LDG and MDG ($p = 0.0048$; $p < 0.001$), and the percentage of T2-type cells increased with the dose of infection. At 24 weeks, the percentage of T2 cells was higher in HDG than in LDG ($p = 0.0014$).

Dynamic changes of T17-type CD4 T cells in the liver of mice with different *E. granulosus s.s.* PSC inocula.
T17-type CD4+ T cells (CD4+IL-17A+) were investigated in the liver (Fig. 5 and Supplementary Fig. S4). In LDG, T17-type cell percentage was significantly lower at 12 weeks than at 2 weeks and 24 weeks ($p = 0.0293$; $p = 0.0365$). In HDG, T17-type cell percentage was significantly higher at 2 weeks than at 12 weeks and 24 weeks ($p < 0.001$; $p < 0.001$).

At 2 weeks, the percentage of T17-type cells was significantly higher in HDG than in LDG and MDG ($p = 0.0043$; $p < 0.001$).

Dynamic changes of Treg-type CD4 T cells and CD8 T cells in the liver of mice with different _E. granulosus s.s._ PSC inocula. Treg-type CD4$^+$ T cells (CD4$^+$CD25$^+$Foxp3$^+$, CD4$^+$IL-10$^+$) and regulatory CD8$^+$ T cells (CD8$^+$IL-10$^+$) were investigated in the liver (Fig. 5 and Supplementary Fig. S4). In HDG, Treg-type CD4$^+$ T cell percentage was significantly higher at 24 weeks than 12 weeks ($p = 0.0016$). CD8$^+$IL-10$^+$ T cells percentage was not significantly different in the three groups.

At 24 weeks, Treg-type CD4 T cells (CD4$^+$CD25$^+$Foxp3$^+$) percentage was significantly higher in HDG than that in in the control group ($p = 0.0486$). At 2 weeks, CD8$^+$IL-10$^+$ T cells percentage was significantly higher in LDG and MDG than that in the control group ($p = 0.0144$; $p = 0.0223$).

Discussion

Hydatid (CE) cysts, the larval stage of _E. granulosus s.s._, are able to survive in tissues, particularity in the liver of human hosts for long periods of time, often causing chronic infection[17]. The cellular distribution and phenotypes of immune mediators in the liver are distinct from those found in the periphery; analysis at the site of infection is thus key to deciphering anti-_E. granulosus s.s._ immunity. Immune responses elicited in the liver during experimental secondary infection by _E. granulosus s.l._, especially those observed at an early stage of infection, have been far less studied than those observed in _E. multilocularis_ infection[12]. The aim of this study was to develop a suitable experimental model that mimics naturally infected livers to comprehensively investigate how the parasite load affects the quality of local immune response of the anti-_E. granulosus s.s._ and the outcome of the larval parasitic infection.

Consistent with previous data[18], our study documented that mice were suitable hosts for secondary CE using PSCs obtained from sheep, and the hydatid cysts developing in the liver actually resembled those of naturally infected human liver in CE and those obtained in Balb/cJ and DBA/2 J mice by using eggs through the oral route[19]. Alternative models to peroral ingestion of eggs have been proposed in the past. Peritoneal and intravenous injections of _E. granulosus_ eggs or oncospheres were proposed by Dempster _et al._ in 1991[19]: when activated oncospheres were injected intraperitoneally into Balb/cJ, DBA/2 J and CF-1 mice, cysts were restricted to the peritoneal cavity; activated oncospheres injected intravenously, however, lodged almost exclusively in the lung and thoracic cavity, except in DBA/2 J mice where 55% lodged in the liver. Different strains also exhibited different susceptibilities to secondary CE[20,21]. Our model of PSC injection has also the particular advantage of accurately mimickings secondary echinococcosis caused by local protoscolex spillage in the liver after spontaneous or therapeutic rupture of the cysts in humans. With this model, the cysts developed at a similar rate as after intraperitoneal (i.p.) inoculation with oncospheres, and macroscopic observations of the livers from our different dose groups were similar to those of the primary infection model[19]. After 4 weeks of infection, the cysts were located both at the surface of and in the liver lobes. This confirmed the initial observations made by Sahin _et al._[22] who established a model via the peripheral branch of the mesenteric vein; compared to that technique, the direct intraportal vein injection seems easier to perform and well reproducible. The most striking difference between the course of _E. granulosus s.s._ and _E. multilocularis_ development to mature metacestodes in the same model of intra-portal injection was the absence of dose-dependent development when using _E. granulosus s.s._ PSCs. After _E. multilocularis_ infection through the same route[9], the establishment of typical _E. multilocularis_ lesions was proportional to the PSC load. In fact, after _E. granulosus s.s._ PSC portal injection, macroscopic and histological examination demonstrated that at the early stage of infection (2 and 4 weeks), all infected mice, whatever the parasite load, showed minute foci in the liver caused by the parasite, thus were actually infected; however, at the middle and later stages (after 4 weeks), the foci almost disappeared and most of them healed, without significant fibrosis; only a small percentage of _E. granulosus s.s._ PSCs were able to develop into defined CE cysts in the different dose groups, but they did develop in all groups of mice, including those receiving the lowest dose, and they were surrounded by a fibrotic AL. Such observations were previously reported in models using intraperitoneal or intravenous routes[23]. Except for the CE cysts formation, the granulomatous inflammatory responses was the most frequent pathological changes, which was in agreement with the results reported by Díaz _et al._[24], in which the granulomas were classified into different types. To our knowledge, this is the first time that such a course of lesions in the liver is formally described. These observations highly suggested that local cellular immunity and fibrosis were actually protective and partially able to limit or even clear PSCs in the liver; however, low antigenic stimulation was not able to trigger a totally protective host's immune response, as it apparently did after _E. multilocularis_ PSC injection, and some of the PSCs could always partially escape protective immunity and develop into cysts. Such an observation partly explains the differences in incidence of the 2 diseases in areas endemic both for AE (rarer) and CE (more frequent) despite the same definitive host (dogs) and similar levels of infectious eggs in the environment, as it happens in Western China[25].

The terms 'establishment' and 'established' phases have been proposed to describe the developmental events occurring from the oncosphere to fully formed metacestodes and the events after metacestode formation respectively[26]. Such terms may also qualify the situation encountered in our model, in which metacestode formation comes from PSCs butnot from oncospheres. Our observations at 2 weeks fit with the definition of the 'establishment' phase. From the 12th week the metacestodes were definitely in the 'established phase' in most of experimental mice. However, at the 4th week, at least one metacestode (of the HDG group) was actually in the established phase, and at the 8th week, several metacestodes were already in the established phase, although anumber of them were still in the establishment phase, even in the same liver, and in the same dose group, which supported the suggestion by Mourglia-Ettlin _et al._ of a more complex parasite-host relationship than previously anticipated[26]. Evaluation of the immune cells in the establishment phase, whatever the dose-related group, showed that this phase was characterized by host's cell granulomatous infiltration at the sites of PSCs in the liver, similar to that observed at the post-oncospheral stage in the 'natural' mode of infection[26]; the presence of CD19$^+$ B cells, CD4$^+$ T and CD8$^+$ T confirmed the combined role of complement-activating anti-_Echinococcus_ specific antibodies and of cellular immunity at that stage[21,26]; however, the early T2 profile, observed in all groups at 2 weeks, and especially

marked in the group with high PSC load, together with a high Th17 profile in this group, as well as the early presence of CD8+IL-10+ T cells, suggested that part of CD4+ T and CD8+ T cells have a regulatory function and could play a role in the survival and growth of PSCs whatever the injection dose, especially in the high dose group; it may also be involved in the number of maturing cysts in each mouse, at later stages, which was weakly related to the parasitic load. The 4–8 week-stage thus appeared to be a crucial 'intermediate (or transitional)' phase which could correspond to an early or more delayed formation of the LL, susceptible to protect the developing GL of the cyst against further host's response by tolerance induction, to allow cyst growth, and to prevent extra-cellular matrix remodelling at its contact, with the persistence of a fibrous AL around the parasitic cyst. At the established phase, the absolute numbers of NK, NKT and B cells were significantly increased in the liver of HDG mice, as was observed in previous studies after i.p. infection of mice with PSCs[26–28], suggesting a role for NK cells in the control of mature cysts. Similar studies in CE patients had also shown that CD3+ T cells, CD3+CD56+ natural killer T cells (NKT) and B cells were the most frequent infiltrating cells at the periphery of hepatic CE lesions; the predominance of CD3+-immunostained cells with weak expression of CD4+ and CD8+ subtypes in CE biopsies also highlighted the role CD3+CD56+NKTs in the partial protection towards *E. granulosus* metacestode growth by the host's immune system; it might be involved in the differences in cyst size we observed between the LDG and the HDG[29]. The persistent presence of B cells suggested a secretion of antibodies by local B cells in the liver[20]; this could explain why specific antibodies (used for CE diagnosis) are more frequently found in patients with liver cysts than in lung cysts where the AL is less cellular[3].

Pathological aspects of lesions in the *E. multilocularis* and in *E. granulosus s.s.* models respectively mimicked the notably different pathological aspects observed in AE and CE[3], and, as stressed above, the outcome of *E. granulosus s.s.* infection in LDG and MDG was markedly different from that of *E. multilocularis* we reported previously, since in LDG and MDG *E. multilocularis* growth was fully cleared or considerably limited, while most of the mice of the HDG developed chronic infection[9]. In previous studies of *E. multilocularis*-infected mice, rapid inactivation of the metacestode at the very early stages, with the constitution of inflammatory and fibrotic foci morphologically similar to those observed in our *E. granulosus s.s.* model, was only observed when mice were pre-treated either with IL-12[30] or IFN-alpha-2a[31,32], that enhance T1-type immunity at the first stages of metacestode formation. This suggests that, despite our observations of a dominant CD8 T cell-related regulatory profile at 2 weeks, a strong stimulation of innate immunity leading to a strong T1 component of the immune response was present earlier, at the very initial stage of *E. granulosus s.s.* PSC development into metacestode, a stage that we missed in our experiments and that should be studied specifically. The absence of relationship between parasite load and the development of the AL raises complementary questions which should be addressed in further works. A definite relationship between parasite load and cytokine responses was previously shown in another experimental model of secondary CE[33]; our results with portal vein injection in C57BL/6 mice were in agreement with such previous reports, which are considered closer to the human situation in terms of resistance/susceptibility.

On comparing T cell subsets and cytokine production observed in the present study with those of *E. multilocularis* infection[9], we could not figure out major differences in the immune cell homing and cytokine profiles between both infections; such a failure has already been stressed by reviews aimed at comparing the immune response towards both cestodes. We nevertheless observed that they exhibited some differences, summarized in Supplementary Fig. S5 for LDG, MDG and HDG respectively. At the early 'establishment' phase (2 weeks), the CE model presented with sequential and combined T1, T17-type T cells and Treg (CD8+IL-10+) profiles even in the LDG, while the AE model exhibited more dominant T1 and T17-type T cells subsets, associated with a nearly total parasite clearance in the LDG. In the intermediate and established phases (12 and 24 weeks), the CE model presented with a mixed T1 (CD4+IFN-γ+, CD8+IFN-γ+), T2, and T17-type T cell profile in all different dose groups, while the AE model exhibited T1 (CD4+IFN-γ+, CD8+IFN-γ+ and CD8+TNF-α+), T2 and Treg (CD4+IL-10+, CD8+IL-10+) profiles mostly in the HDG. Among the factors that could determine both a different type of stimulation of the various types of immune response and differences at the microenvironment level, the nature of the LL in *E. granulosus s.l.* and in *E. multilocularis* respectively is a major candidate[12]. Previous studies have shown that the *E. multilocularis* LL is probably formed by a single type of mucin backbone, while a second apomucin subfamily additionally contributes to *E. granulosus s.s.* LL[34,35]. In CE, the LL seems to prevent the exogenic budding that characterizes AE lesions; in addition, as complement-activating antibodies are part of the protective immune response[36], LL represents a first barrier against the host's immune attack; in addition, we may hypothesize that its composition may attract and trigger the activation of the host's cells involved in the development of the AL, which constitutes a second barrier when the cyst is fully established[12]. Different excretory/secretory metabolic products have been identified in the HF of *E. granulosus s.s.* and *E. multilocularis* respectively; recent research has shown that the presence of more enzymes in *E. granulosus s.s.* HF might be correlated with longer survival of *E. granulosus s.s.* metacestode compared to *E. multilocularis* because of an advantage in energy sources and by the protection they ensure to the parasite from the host's immune system[37]. Progress in proteomics and in the study of differential gene expression[38] should make the combined comparison of *E. multilocularis* and *E. granulosus s.s.* LL and HF and of the host's immune response possible, at the very initial stages and at the single lesion level by using the quantitative intrahepatic portal vein model now well established for the two species.

Materials and Methods

Ethics approval and consent to participate.
All mice received humane care and were used in all course of experiment according to the Animal Ethics Procedures and Guidelines of the People's Republic of China (Regulations for Administration of Affairs Concerning Experimental Animals, China, 1988). The animal experiment was approved by The Animal Care and Use Committe and the Ethical Committe of First Affiliated Hospital of Xinjiang Medical University (20140411-05). All methods were performed in accordance with the relevant guidelines and regulations.

Animal model and procedures.   Female specific pathogen-free C57BL/6 mice of 8–10 weeks of age were obtained from the Beijing Vital River Experimental Animal Technology Co. Ltd. and were kept in the specific pathogen-free animal facility of the Research Center of the First Affiliated Hospital of Xinjiang Medical University.

E. granulosus s.s. PSCs were isolated from fresh sheep liver obtained from a local slaughterhouse, and rinsed 10 times with phosphate buffered saline, pH = 7.2, containing 1000 mg/mL penicillin and 1000 U/mL streptomycin (Hyclone,Beijing, China). Only *E. granulosus s.s.* PSCs inocula with a vitality over 95% confirmed by 1% methylene blue exclusion were used for portal injection in mice. The mice in experimental group were injected with different doses of PSCs via portal vein and portal saline injection was defined as control group. A middle abdominal incision was made in mice under anaesthetic and 200–300 μL of PSCs sediment or saline was injected via portal vein by using a 0.45 × 15RWLB venous infusion needle. After injection, a cotton bud was pressed on the puncture site for 5 min to provide haemostasis and to prevent intraperitoneal spillage of the PSCs. The abdominal cavity was then closed and then the mice were put on the warm stage to promote waking.

Definition.   To determine whether the infection percentage (or the cyst numbers) were directly related to infection dose, the mice were divided into low dose group (LDG, 50 PSCs and 250 PSCs injected through the portal vein), medium dose group (MDG, 500 PSCs), and high dose group (HDG, 1000 PSCs and 2000 PSCs).

4–6 mice in per group were sacrificed at 2, 4, 8, 12, 16, 20 and 24 weeks. Based on histological aspects and our previous research on *E. multilocularis*[9], we selected the groups inoculated with 50 (LDG), 500 (MDG) and 2000 (HDG) PSCs to study their immune response at 2 weeks (early stage), 12 weeks (middle stage) and 24 weeks (later stage) after infection, as to further explore the correlation between inoculum doses, development of parasite-induced immune response, and resistance to infection.

The mean number (No.) cysts was defined as the total number of cysts divided by the number of mice. The infection percentage was defined as the number of infected mice with cysts, divided by number of mice in the group, multiplied by 100[19]. The formation ratio of the cysts was defined as the total number of cysts divided by the number of PSCs and the number of mice per group [total number of cysts/(number of PSCs × number of mice)], according to the previous reports[33].

Tissue sampling and histopathological analysis.   Sixmouse hepatic lobes were separated and put in the 4% buffered formalin for 2 days, then dehydrated overnight, and finally embedded in paraffin. Paraffin-embedded 4 μm sectionson glass slides were stained with Hematoxylin-Eosin to study inflammatory cells infiltration and granuloma and hepatic cyst formation. Histological reactions were defined as four types: (1) inflammatory foci, parasite-free, except for possible PSC remnants, composed of macrophages, lymphocytes, and other inflammatory cells; (2) fibrotic foci, parasite-free, with no visible PSCs or cysts, only composed of fibrosis, without cell infiltrates; (3) inflammatory foci with fibrosis, parasite-free, with no visible PSCs or cysts, only composed of granulomatous inflammation combined with liver fibrosis; (4) infectious foci, cystic structure composed of the GL and LL, surrounded with macrophages, lymphocytes, fibroblasts, myofibroblasts, as well as fibrosis (AL). The various parameters were measured, expressed, and analysed as previously described[9].

For liver fibrosis detection, paraffin-embedded 5 μm sections were stained with picric acid-Sirius red and anti-alpha smooth muscle actin antibody to respectively evaluate collagen fibers and myofibroblasts, as described previously[39].

Liver mononuclear cell isolation and flow cytometry analysis.   Leukocytes were isolated from the liver in the way as described previously[40]. For flow cytometry, cells were stained for surface antigens with anti-NK1.1, anti-CD3, anti-CD4, anti-CD8α, anti-CD19, anti-CD44, anti-CD62L (BioLegend, San Diego, CA), or/and for intracellular antigens with anti-IFN-γ, anti-IL-4, anti-IL-17A, anti-TNF-α and anti-IL-10 (BioLegend). IgG isotype controls (Biolegend) were used in parallel. To detect Treg cells, cells were stained with anti-NK1.1, anti-CD3, anti-CD4, anti-CD25 at 4 °C for 30 minutes; and incubated with anti-mouse Foxp3 antibodies according to the manufacturer's instructions (eBioscience). Methods were the sameas those described previously[9].

Statistical analysis.   Data were expressed as mean ± standard error of the mean and analyzed by GraphPad Prism 7.0 (GraphPad Software, San Diego, CA). The one-way ANOVA test with a Tukey's multiple comparison was used to test comparisons among multiple groups and the Student's t -test was used to test comparisons between two groups, after checking for the normality of the data. If the individual values of the population were not a normal distribution and (or) unequal variances, non-parametric tests (Kruskal-Wallis test) wereused to test comparisons among groups. Correlation analysis (linear correlation) was used to test correlation between two variables. The p-value less than 0.05 was defined as a significant difference in this study (p-values were expressed in the figures as follows: *p values < 0.05; **p values < 0.01; ***p values < 0.001). Onlythose results which were statistically significant were reported in the Results section. Allresults are shown in the tables and figures.

Ethics approval and consent to participate.   All mice received humane care in all course of experiment. The animal experiment was approved by The Animal Care and Use Committe and the Ethical Committe of First Affiliated Hospital of Xinjiang Medical University (20140411-05).

Data availability
The datasets generated during and/or analysed during the current study are available from the corresponding author on reasonable request.

References

1. Deplazes, P. *et al*. Global Distribution of Alveolar and Cystic Echinococcosis. *Advances in parasitology* **95**, 315–493 (2017).
2. Torgerson, P. R. & Macpherson, C. N. The socioeconomic burden of parasitic zoonoses: global trends. *Veterinary parasitology* **182**, 79–95 (2011).
3. Kern, P. *et al*. The Echinococcoses: Diagnosis, Clinical Management and Burden of Disease. *Advances in parasitology* **96**, 259–369 (2017).
4. Siles-Lucas, M., Casulli, A., Cirilli, R. & Carmena, D. Progress in the pharmacological treatment of human cystic and alveolar echinococcosis: Compounds and therapeutic targets. **12**, e0006422 (2018).
5. Brunetti, E., Kern, P. & Vuitton, D. A. Expert consensus for the diagnosis and treatment of cystic and alveolar echinococcosis in humans. *Acta tropica* **114**, 1–16 (2010).
6. Zhang, Q. *et al*. Role of immune tolerance in BALB/c mice with anaphylactic shock after Echinococcus granulosus infection. *Immunologic research* **64**, 233–241 (2016).
7. Rigano, R. *et al*. Echinococcus granulosus antigen B impairs human dendritic cell differentiation and polarizes immature dendritic cell maturation towards a Th2 cell response. *Infection and immunity* **75**, 1667–1678 (2007).
8. Mourglia-Ettlin, G., Marques, J. M., Chabalgoity, J. A. & Dematteis, S. Early peritoneal immune response during Echinococcus granulosus establishment displays a biphasic behavior. *PLoS neglected tropical diseases* **5**, e1293 (2011).
9. Zhang, C. *et al*. T-cell tolerance and exhaustion in the clearance of Echinococcus multilocularis: role of inoculum size in a quantitative hepatic experimental model. *Scientific reports* **7**, 11153 (2017).
10. Zhang, R. *et al*. Nanosecond pulsed electric field (nsPEF) disrupts the structure and metabolism of human Echinococcus granulosus protoscolex *in vitro* with a dose effect. *Parasitology research* **116**, 1345–1351 (2017).
11. Zhang, R. Q., Chen, X. H. & Wen, H. Improved experimental model of hepatic cystic hydatid disease resembling natural infection route with stable growing dynamics and immune reaction. *World journal of gastroenterology* **23**, 7989–7999 (2017).
12. Gottstein, B. *et al*. Immunology of Alveolar and Cystic Echinococcosis (AE and CE). *Advances in parasitology* **96**, 1–54 (2017).
13. Siracusano, A. *et al*. Immunomodulatory mechanisms during Echinococcus granulosus infection. *Experimental parasitology* **119**, 483–489 (2008).
14. Tsai, I. J. *et al*. The genomes of four tapeworm species reveal adaptations to parasitism. *Nature* **496**, 57–63 (2013).
15. Zheng, H. *et al*. The genome of the hydatid tapeworm Echinococcus granulosus. *Nature genetics* **45**, 1168–1175 (2013).
16. Liu, C. N. *et al*. Discrimination between E. granulosus sensu stricto, E. multilocularis and E. shiquicus Using a Multiplex PCR Assay. *PLoS neglected tropical diseases* **9**, e0004084 (2015).
17. Brunetti, E., Garcia, H. H. & Junghanss, T. Cystic echinococcosis: chronic, complex, and still neglected. *PLoS neglected tropical diseases* **5**, e1146 (2011).
18. Yin, J., Liu, C., Shen, Y., Zhang, H. & Cao, J. Efficacy of ursolic acid against Echinococcus granulosus *in vitro* and in a murine infection model. *Parasites & vectors* **11**, 58 (2018).
19. Dempster, R. P., Berridge, M. V., Harrison, G. B. & Heath, D. D. Echinococcus granulosus: development of an intermediate host mouse model for use in vaccination studies. *International journal for parasitology* **21**, 549–554 (1991).
20. Mourglia-Ettlin, G., Cucher, M., Arbildi, P., Rosenzvit, M. & Dematteis, S. Natural and induced antibodies contribute to differential susceptibility to secondary cystic echinococcosis of Balb/c and C57Bl/6 mice. *Immunobiology* **221**, 103–115 (2016).
21. Mourglia-Ettlin, G., Merlino, A., Capurro, R. & Dematteis, S. Susceptibility and resistance to Echinococcus granulosus infection: Associations between mouse strains and early peritoneal immune responses. *Immunobiology* **221**, 418–426 (2016).
22. Sahin, M., Aydin, A., Bulbuloglu, E. & Ciralik, H. Experimental hydatid disease of the liver. *European journal of clinical investigation* **27**, 537–538 (1997).
23. Zhang, W. *et al*. Immunoglobulin profiles in a murine intermediate host model of resistance for Echinococcus granulosus infection. *Parasite immunology* **25**, 161–168 (2003).
24. Diaz, A., Sagasti, C. & Casaravilla, C. Granulomatous responses in larval taeniid infections. *Parasite immunology* **40**, e12523 (2018).
25. Craig, P. S. *et al*. Prevention and control of cystic echinococcosis. *The Lancet. Infectious diseases* **7**, 385–394 (2007).
26. Mourglia-Ettlin, G. *et al*. Echinococcus granulosus glycoconjugates induce peritoneal B cell differentiation into antibody-secreting cells and cytokine production. *Parasite immunology* **33**, 621–631 (2011).
27. Dematteis, S. *et al*. Antibody and Th1/Th2-type responses in BALB/c mice inoculated with live or dead Echinococcus granulosus protoscoleces. *Parasite immunology* **21**, 19–26 (1999).
28. Yanagita, M. *et al*. Nasopharyngeal-associated lymphoreticular tissue (NALT) immunity: fimbriae-specific Th1 and Th2 cell-regulated IgA responses for the inhibition of bacterial attachment to epithelial cells and subsequent inflammatory cytokine production. *Journal of immunology (Baltimore, Md.: 1950)* **162**, 3559–3565 (1999).
29. Vatankhah, A. *et al*. Characterization of the inflammatory cell infiltrate and expression of costimulatory molecules in chronic Echinococcus granulosus infection of the human liver. *BMC infectious diseases* **15**, 530 (2015).
30. Emery, I., Leclerc, C., Sengphommachanh, K., Vuitton, D. A. & Liance, M. *In vivo* treatment with recombinant IL-12 protects C57BL/6J mice against secondary alveolar echinococcosis. *Parasite immunology* **20**, 81–91 (1998).
31. Harraga, S. *et al*. Clinical efficacy of and switch from T helper 2 to T helper 1 cytokine profile after interferon alpha2a monotherapy for human echinococcosis. *Clinical infectious diseases: an official publication of the Infectious Diseases Society of America* **29**, 205–206 (1999).
32. Godot, V. *et al*. IFN alpha-2a protects mice against a helminth infection of the liver and modulates immune responses. *Gastroenterology* **124**, 1441–1450 (2003).
33. Dematteis, S., Rottenberg, M. & Baz, A. Cytokine response and outcome of infection depends on the infective dose of parasites in experimental infection by Echinococcus granulosus. *Parasite immunology* **25**, 189–197 (2003).
34. Del Puerto, L. *et al*. Negligible elongation of mucin glycans with Gal beta1-3 units distinguishes the laminated layer of Echinococcus multilocularis from that of Echinococcus granulosus. *International journal for parasitology* **46**, 311–321 (2016).
35. Diaz, A. *et al*. The laminated layer: Recent advances and insights into Echinococcus biology and evolution. *Experimental parasitology* **158**, 23–30 (2015).
36. Barrios, A. A. *et al*. Inefficient and abortive classical complement pathway activation by the calcium inositol hexakisphosphate component of the Echinococcus granulosus laminated layer. *Immunobiology* **224**, 710–719 (2019).
37. Ahn, C. S., Kim, J. G., Han, X., Kang, I. & Kong, Y. Comparison of Echinococcus multilocularis and Echinococcus granulosus hydatid fluid proteome provides molecular strategies for specialized host-parasite interactions. *Oncotarget* **8**, 97009–97024 (2017).
38. Wen, H. *et al*. Echinococcosis: Advances in the 21st Century. *Clinical microbiology reviews* **32** (2019).
39. Heinrichs, D. *et al*. The chemokine CCL3 promotes experimental liver fibrosis in mice. *PLoS One* **8**, e66106 (2013).
40. La, X. *et al*. Upregulation of PD-1 on CD4+CD25+T cells is associated with immunosuppression in liver of mice infected with Echinococcus multilocularis. *International Immunopharmacology* **26**, 357–366 (2015).

Acknowledgements

Author contributions

Conceived and designed the experiments: Z.L., C.Z. and H.W.2. Performed the experiments: Z.L., C.Z., X.B., S.Y., H.W.1., L.L.2., N.Z., Y.N., A.A.1. and A.A.2. Analyzed the data: Z.L., C.Z., L.L.1. Wrote the paper: Z.L., C.Z., R.L. and D.V.

Competing interests

The authors declare no competing interests.

Additional information

Supplementary information is available for this paper at https://doi.org/10.1038/s41598-019-56098-3.

Correspondence and requests for materials should be addressed to H.W.

Reprints and permissions information is available at www.nature.com/reprints.

Publisher's note Springer Nature remains neutral with regard to jurisdictional claims in published maps and institutional affiliations.